Natural abundance high field 43Ca NMR solid state NMR in cement science

Moudrakovski, I.; Alizadeh, R.; Beaudoin, J. J.

Publisher's version / Version de l'éditeur:
https://doi.org/10.1039/c000353k
Physical Chemistry Chemical Physics, 12, pp. 6961-6969, 2010-06-01

Natural abundance high field ^{43}Ca NMR solid state NMR in cement science

NRCC-53542

Moudrakovski, I.; Alizadeh, R.; Beaudoin, J.J.

June 2010

A version of this document is published in / Une version de ce document se trouve dans:
Physical Chemistry Chemical Physics, 12, pp. 6961-6969, June 01, 2010, DOI: 10.1039/c000353k

Natural abundance high field ^{43}Ca solid state NMR in cement science†

Igor L. Moudrakovski,*[a] Rouhollah Alizadeh[b] and James J. Beaudoin[b]

Received 7th January 2010, Accepted 11th March 2010
First published as an Advance Article on the web 12th May 2010
DOI: 10.1039/c000353k

This work is a systematic attempt to determine the possibilities and the limitations of the ^{43}Ca high field solid state NMR in the study of cement-based materials. The low natural abundance (0.135%) and small gyromagnetic ratio of ^{43}Ca present a serious challenge even in a high magnetic field. The NMR spectra of a number of cement compounds of known structure and composition are examined. The spectra of several phases important in cement science, *e.g.*, anhydrous beta di-calcium silicate (β-C_2S) and tri-calcium (C_3S) silicate were obtained for the first time and the relation of spectroscopic and structural parameters is discussed. The method was also applied to the hydrated C_3S and synthetic calcium silicate hydrates (C–S–H) of different composition in order to understand the state of calcium and transformations in the structure during hydrolysis. The spectra of hydrated C_3S reveals a calcium environment similar to that of the C–S–H samples and 11 Å Tobermorite. These observations support the validity of using layered crystalline C–S–H systems as structural models for the C–S–H that forms in the hydration of Portland cement.

Introduction

Cement is a primary construction material with an annual production and consumption in billions of tons. Considering the great demand for this material, it would be difficult to overestimate the importance of a deep understanding of its structure and detailed knowledge of the relevant chemical transformations (that occur during hydrolyses). It was estimated, that the cement industry contributes to about 5% of the global CO_2 emissions, making it an important sector for CO_2-emission mitigation strategies.[1] Understandably, even minor improvements in the technological process of cement production will lead to a significant saving in energy. The same can be argued about development of cements with improved properties and various additives that lower the amounts of cement in concrete and increase its quality.

Solid state nuclear magnetic resonance (SS NMR) is one of the major spectroscopic techniques that has played a significant role in studies of cement-based materials and processes. Until recently, most of the SS NMR studies concentrated on nuclei such as ^{29}Si, ^{27}Al, ^{17}O and ^{1}H. All of these nuclei are important in the nanostructural studies of cementitious materials. The investigations in this regard have provided a wealth of information regarding the inter-connectivity of the atoms in the framework and processes of hydrolysis.[2–15] Several comprehensive reviews summarizing SS NMR applications in cement[16–18] and silicate[19] research are currently available. The main strength of the method is rooted in its sensitivity to the local environment of the atoms. In a broad sense the method is complementary to the XRD, and can also be used in the studies of amorphous and semi-crystalline materials.

The properties of cement compounds and hydrated phases depend greatly on the coordination and local environment of calcium atoms. ^{43}Ca solid state (SS) NMR could therefore potentially play a significant role in structural and chemical studies of these materials. Recent studies have demonstrated impressively that the technique is suitable for resolving complicated structural problems not accessible by other methods.[20,21] ^{43}Ca has a chemical shift range of nearly 200 ppm, reflecting the sensitivity to the chemical environment of calcium.[22] Correlations between the mean Ca–O distance in the polyhedron and the chemical shift of ^{43}Ca have been reported.[23,24] An important factor in interpreting and assigning the chemical shifts in the spectra also comes from the latest development in computational methods of NMR parameters. The most notable progress in recent years was achieved in calculations of periodic structures such as occur in crystalline materials.[25] In many situations chemical shielding and quadrupolar parameters can be calculated with very high accuracy and reliability.[20,24] Despite its advantages, the application of ^{43}Ca SS NMR in materials chemistry has been limited with just twenty original publications on the subject produced during the past 15 years.[20,21,23–44]

The roots of the problem are mainly due to the great difficulties in obtaining the spectra. The only magnetically active isotope ^{43}Ca has a low natural abundance of only 0.135% and is a spin 7/2 quadrupolar nuclei with a rather small magnetogyric ratio γ (absolute resonance frequency Ξ = 6.7299 MHz) and a moderate quadrupolar moment of −4.08 fm^2. The miniscule natural abundance and low resonance frequency complicated by quadrupolar interactions make ^{43}Ca SS NMR a challenging exercise. When the calcium is not in a highly symmetric environment, *i.e.* as in cubic calcium oxide, the observed signal of the central transition is

[a] *Steacie Institute for Molecular Sciences, National Research Council, Ottawa, ON, Canada K1A 0R6*
[b] *National Research Council of Canada, Institute for Research in Construction, 1200 Montreal Rd, Ottawa, ON, Canada K1A 0R6*

† Electronic supplementary information (ESI) available: Correlation between experimental ^{43}Ca chemical shifts and calculated absolute shieldings and Table of calculated NMR parameters for triclinic C_3S. See DOI: 10.1039/c000353k

commonly broadened by the second order quadrupolar interaction,[45,46] drastically reducing the intensity of the signals. An additional complication commonly encountered in solid state NMR of low-γ nuclei is rather long relaxation times. In the case of ^{43}Ca, T_1's as long as tens of seconds can be expected,[20,24] seriously complicating accumulation of the signals.

In the case of calcium silicates, the difficulty is magnified by the large variety of the structural environments calcium can be found in. In practice, it leads to spreading the total intensity among multiple signals and resulting in an overall low intensity. The NMR of amorphous materials will be the most affected; it can however be a serious problem even in crystalline materials. Great difficulties of ^{43}Ca SS NMR were demonstrated in a recent study,[42] where attempts were made to obtain the spectra of synthetic calcium silicate hydrate minerals including Tobermorite and Jennite. Working at the magnetic field of 21.1 T, the authors were able to obtain only marginally usable spectra after two full days of acquisition. Tobermorite and Jennite minerals are considered as model compounds for the calcium silicate hydrate (C–S–H‡) in Portland cement and C_3S paste which is a nearly amorphous material. C–S–H is the principal product in the hydration of calcium silicate phases of Portland cement, *i.e.* β-C_2S and C_3S.

Tricalcium silicate (C_3S) is the main clinker phase of the Portland cement. C_3S is known to have 29 distinct Ca sites in its triclinic form[47] and 36 sites in the monoclinic superstructure.[48] Even if some of these sites incidentally have indistinguishable signals and completely overlap, the overall ^{43}Ca NMR spectrum is expected to be very complicated. The hydrated calcium silicate, *i.e.* C–S–H, is primarily responsible for important properties such as strength in hardened cement-based materials. The hydration mechanism of C_3S and the nanostructure of the C–S–H are central to the understanding of the chemical and physical characteristics of cement-based materials. Despite decades of research on the nature of C–S–H, the debate over its nanostructure still continues.[49,50] Understanding the mechanism of cement hydration and properties of the principal component in cement paste, C–S–H, provides an opportunity for practical modification and improvement of cement systems in the future.

This work is an attempt at a systematic ^{43}Ca SS NMR study of cement-based materials aimed at defining the possibilities and the limitations of the method in this discipline. First, the spectra of the anhydrous cement related compounds of known structure and composition are examined. Second, the method is applied to the hydrated C_3S and synthetic C–S–H samples of different composition in order to elucidate the state of calcium and transformations in the structure during hydrolysis.

Experimental and theoretical methods

Materials

The materials investigated in the current study all have a natural abundance of the ^{43}Ca isotope and were either commercially available or synthesized in the course of this work. The cement clinker phases including C_3S (triclinic and monoclinic), β-C_2S and C_3A were obtained from the CTL group (Skokie, IL). Three C–S–H samples (C/S ratio = 0.8, 1.2 and 1.5) were synthetically prepared from the reaction between stoichiometric amounts of CaO and SiO_2 in excess water. CaO was freshly produced from the calcination of $CaCO_3$ (Sigma-Aldrich) at 900 °C. Amorphous silica (Cab-*O*-Sil, Type M-5) was obtained from Cabot Inc. Details of the C–S–H synthesis can be found elsewhere.[51] The synthetic C–S–H with a C/S ratio below 1.5 is usually referred to as C–S–H (I). The synthetic C–S–H is semi-crystalline (X-ray *d*-spacings at 1.25, 0.31, 0.28 and 0.18 nm). The amorphous C–S–H formed in hydrated cement is sometimes referred to as 'C–S–H gel' to distinguish the material formed in cement, C_3S or β-C_2S pastes from other varieties of C–S–H. The triclinic C_3S was fully hydrated (at a water/C_3S mass ratio of 0.4) in order to produce C–S–H for comparison with the C–S–H (I). The ^{43}Ca NMR of reagent grade CaO and $Ca(OH)_2$ (Sigma-Aldrich) were examined for comparison with cement-based materials. The 11 Å Tobermorite was synthesized from the hydrothermal reaction of calcium hydroxide and silica fume (having a molar C/S ratio of 0.83) at 180 °C.

NMR measurements

The ^{43}Ca NMR measurements were performed at 60.58 MHz on a Bruker Avance-II 900 MHz instrument (magnetic field of 21.14 T). The magic angle spinning (MAS) experiments were performed using a Bruker single channel 7 mm low-γ probe with dry nitrogen as a carrier gas. A simple single-pulse sequence was used to acquire the spectra. The solution $\pi/2$ pulse was 9 μs and the corresponding selective solid $\pi/2$ pulse was scaled by a factor of four to 2.25 μs. All isotropic chemical shifts are referenced to a 1 M solution of $CaCl_2$ set to 0 ppm. The choice of the reference here is different from that reported in the earlier works[23,26–30] due to the problems associated with the use of saturated solution of $CaCl_2$ as a chemical shift reference.[20,24]

Supplementary ^{29}Si MAS NMR spectra were obtained from the cement clinker silicate phases. This test was carried out on a Bruker Avance 200 MHz instrument (magnetic field of 4.7 T and ^{29}Si Larmor frequency of 39.75 MHz) using a BL7 double resonance MAS probe and 7 mm ZrO_2 spinners at the spinning speed of 5000 Hz. The spectra were acquired in a Bloch decay mode (^{29}Si $\pi/2$ pulse of 4 μs) with a high power composite pulse proton decoupling at a delay of 60 s between scans.

Details of first principles computations

The plane wave based density functional theory calculations of nuclear magnetic shielding and electric field gradient tensors were performed using the NMR module of the CASTEP DFT code[52] that employs the gauge including projector augmented wave (GIPAW) algorithm[53] and is a part of the Accelrys Materials Studio simulation and modeling package.[54] The Perdew Burke Ernzerhof (PBE) functional was used with the generalized gradient approximation (GGA) for all calculations.[55] The convergence of calculated NMR parameters on the size of a Monkhorst–Pack *k*-point grid and a basis set

‡ Cement chemistry nomenclature: C═CaO, S═SiO_2, H═H_2O, A═Al_2O_3. Hyphens in C–S–H indicate no specific stoichiometry are applied.

cut-off energy were tested for all systems. The sufficient basis set cut-off energies were 550 eV and the k-point spacing was always less than 0.04 $Å^{-1}$. Unit cell parameters and atomic coordinates were taken from the most recent published structures as indicated further in the text.

The calculations produce the absolute shielding tensors and the electric field gradients in the molecular frame. The calculated quadrupolar constants are found according to $C_q = eQ - V_{zz}/h$, where Q is the ^{43}Ca quadrupolar moment of -4.08 fm^2 and V_{zz} is the largest principal component of the electric field gradient (EFG) tensor. The asymmetry $\eta = (V_{XX} - V_{YY})/V_{ZZ}$, with the EFG tensor components ordered as $|V_{ZZ}| \geq |V_{YY}| \geq |V_{XX}|$. The calculated quadrupolar parameters can be directly compared to the experimental data.

Since all the experiments were performed with magic angle spinning, the only relevant shielding parameter is the isotropic shielding constant representing a trace of the chemical shielding tensor $\sigma_i = 1/3\mathrm{Tr}\{\sigma\}$. The absolute shielding constants obtained in the calculations were converted into the chemical shift scale using an empirical relationship as $\delta_i^{\mathrm{calc.}} = (1129.1 - \sigma_i^{\mathrm{calc.}})/1.1857$, where $\sigma_i^{\mathrm{calc.}}$ is the calculated shielding constant, and the referencing is to 1 M $CaCl_2$. The relationship was obtained by correlating the CASTEP calculated isotropic shielding constants for a series of Ca-containing materials (using the same level of theory) to their experimental ^{43}Ca chemical shifts both obtained in our lab at 21.1 T and from ref. 30. The correlation is illustrated in Fig. S1 of the ESI.† The isotropic shift in this case is related to the shielding as $\sigma_i^{\mathrm{calc.}}(\mathrm{ppm}) = -1.1857 \cdot \delta_i^{\mathrm{exp.}} + 1129.1$ ($R = 0.994$). We note, that the obtained correlation is very close to that reported recently[20] for a somewhat different set of compounds.

Results and discussions

Cement compounds

The ^{43}Ca MAS spectra of several crystalline cement clinker phases are shown in Fig. 1 in comparison to that of CaO. The spectrum of CaO (Fig. 1-a) consists of a very narrow signal, 21 Hz wide, with the chemical shift of 136.1 ppm. The position of the signal is in good agreement with the data reported previously[23] if corrected for the referencing.[20,24] It should be noted that this is the most deshielded calcium site in an oxygen environment ever reported.

The distinct signals observed in the spectrum of β-C_2S (Fig. 1-b) are consistent with the crystal structure of this compound.[56] The maxima of spectral intensities are at about 46 and 29 ppm. These positions, however, are not the isotropic chemical shift since the signals are visibly affected by the second order quadrupolar interactions. Due to the broadening of the signals, it is difficult to produce an accurate simulation of the signals, and the isotropic shift and the quadrupolar parameters resulting from this simulation should be considered only as estimates. The isotropic chemical shifts for the first and the second signals are 53.8 and 33.7 ppm, with the C_q's being 2.98 and 2.41 MHz, and η's of 0.7 and 0.65, respectively. The integrated ratio of the signals is very close to 1 : 1 as expected from the structure. This is the first experimental report of ^{43}Ca for β-C_2S. The experimental data for both signals are in good agreement with the results of our CASTEP calculations ($\delta_i(1)^{\mathrm{calc.}} = 57.9$ ppm, $C_q(1)^{\mathrm{calc.}} = 2.815$ MHz; $\eta(1)^{\mathrm{calc.}} = 0.43$ and $\delta_i(1)^{\mathrm{calc.}} = 36.5$ ppm, $C_q(1)^{\mathrm{calc.}} = 2.098$ MHz; $\eta(2)^{\mathrm{calc.}} = 0.66$) and recently reported computational data.[24] The structure of β-C_2S is known to be built of isolated SiO_4 tetrahedra in an environment of two distinct Ca ions.[53] The calcium atom in site 1, Ca(1) (here and further we use the same notation as in the original crystallographic publications), is coordinated to six oxygen atoms with Ca(1)···O distances ranging from 2.2287 to 2.6475 Å and the average distance d[Ca(1)···O] = 2.4487 Å (as in ref. 24, the average distance is calculated accounting for only oxygen atoms located no further than 2.7 Å). For the Ca(2) the distances range between 2.3852 and 2.6575 Å, and the average is d[Ca(1)···O] = 2.4975 Å.[56] All Ca–O distances for both Ca sites are very irregular, with no local symmetry in the oxygen environment. This observation suggests a significant deviation of asymmetry parameter η from 0. This indeed is observed in experiment and supported by the first principles calculations of the NMR parameters. Previously, it has been suggested that the average Ca–O distances in calcium-oxygen polyhedra within the same family of inorganic calcium compounds (*i.e.* silicates or aluminates) linearly correlate with ^{43}Ca isotropic shifts.[23,24] According to that correlation, the shorter average distance corresponds to a higher chemical shift of Ca. Although the average Ca–O distances for the two sites are close, one may still expect that the site Ca(1) is the one with the higher chemical shift (53.8 ppm), when the second signal at 33.7 ppm belongs to the site Ca(2). One should note, however, that the experimentally observed ^{43}Ca chemical shifts in β-C_2S are visibly higher than one could expect from the previously reported correlation.

Fig. 1-c and 1-d present the ^{43}Ca NMR spectra of the triclinic and monoclinic C_3S samples, respectively. Although the chemical composition of these two samples is nearly identical, their ^{43}Ca spectra show some remarkable differences in resolution of the signals. The monoclinic C_3S exhibits a very broad and asymmetric signal in the range of 40 to 110 ppm (Fig. 1-d). Such a broadening is commonly observed in situations where the distribution of NMR parameters such as chemical shifts and quadrupolar constants is present. Since the monoclinic crystal structure of C_3S has 36 non-equivalent sites for Ca,[48] it wouldn't be too surprising if some small deviations from the perfect lattice produced the observed broadening in the spectrum. The NMR spectrum of the triclinic C_3S, however, has relatively well-separated ^{43}Ca signals appearing in the range between 40 to 140 ppm. At this point only the signal at 136.2 ppm can be unambiguously assigned to CaO impurities. It is interesting that with 29 inequivalent Ca sites in the structure of C_3S,[47] there is still some distinct separation of the signals in the spectrum. Apparently, some calcium environments in the triclinic C_3S are quite similar, resulting only in a limited dispersion of the ^{43}Ca signal.

In order to confirm the structural environment diversity of the triclinic and monoclinic C_3S, the ^{29}Si MAS NMR was conducted (Fig. 2). It is evident that the signals of the monoclinic sample (Fig. 2-a) are substantially broader than

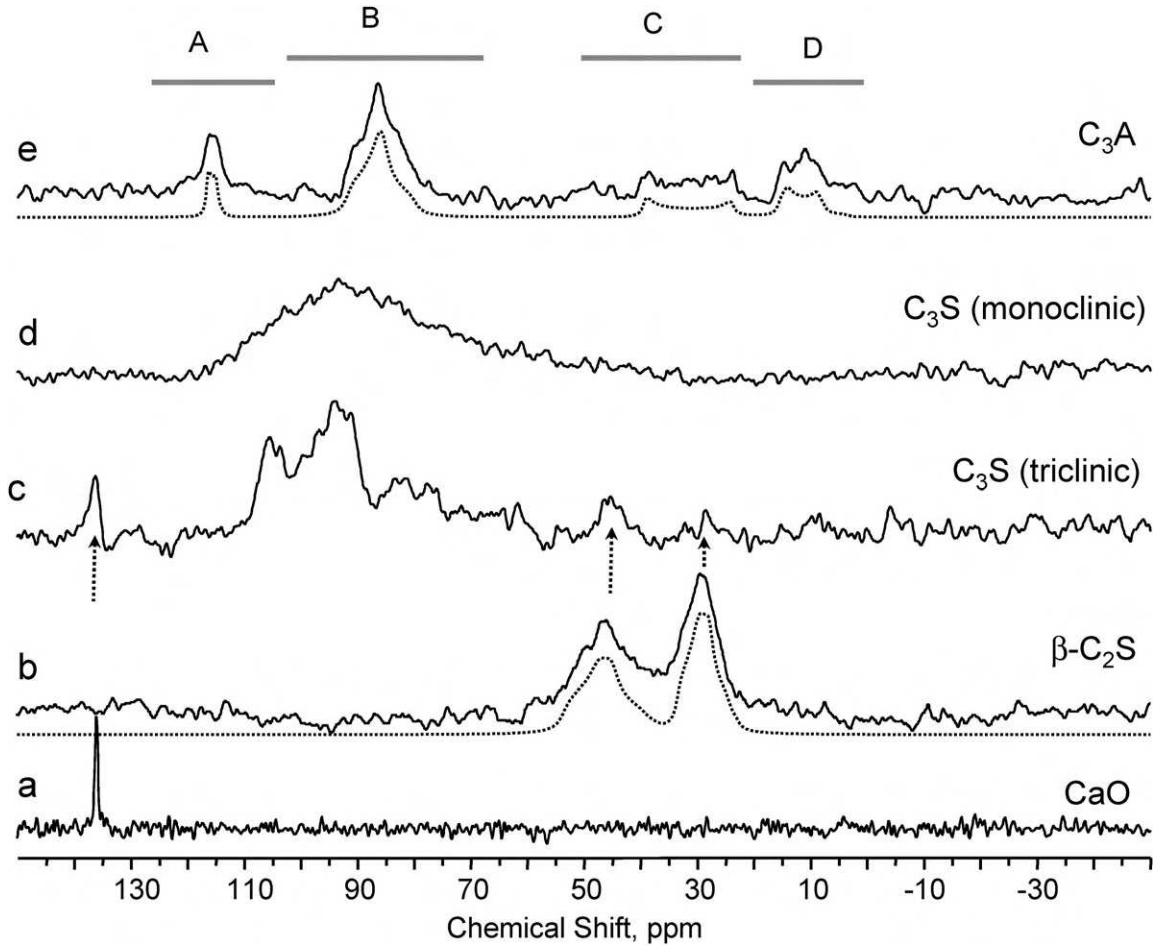

Fig. 1 The natural abundance ^{43}Ca MAS NMR spectra of anhydrous cement based compounds and calcium oxide. Dotted lines below the spectra **b** (β-C_2S) and **e** (C_3A) are the spectral simulations for the second order quadrupolar interactions. The vertical arrows below the spectrum **c** (triclinic C_3S) indicate positions of the signals of CaO and β-C_2S impurities. Regions **A–C** indicating the signals' regions in the spectrum **e** (C_3A) are discussed in the text.

those for the triclinic C_3S (Fig. 2-b). The latter is the type that is usually studied in the literature as it contains well-separated ^{29}Si signals.[57] The monoclinic C_3S has a disordered crystal lattice indicated from the NMR results (both ^{43}Ca and ^{29}Si). This is possibly due to the stabilizers (such as Mg^{2+} and Sr^{2+}) added to the C_3S at high temperatures (above 980 °C) during the formation process in order to preserve the monoclinic state.[58] Otherwise, the produced C_3S would have a triclinic structure. It should also be noted that the alite clinker phase (tricalcium silicate) in Portland cement is substantially composed of monoclinic polymorphs.[58]

The lattice parameters of triclinic C_3S are a = 11.67 Å, b = 12.24 Å, c = 13.72 Å, α = 105.5°, β = 94.33°, γ = 90°, V_{cell} = 2192.84 Å^3,[47] and with eighteen $3CaO{\cdot}SiO_2$ molecules per unit cell this is a serious challenge for periodic structure DFT computational methods.

Nevertheless, the calculations reproduce reasonably well the range of chemical shift that is experimentally observed for Ca sites in alite. Specifically, the calculations predict the spread of the signals between about 40 and 140 ppm with only small fraction of the total intensity located on the edges of the region and the majority of it concentrated between 70 and 105 ppm. The majority of the calculated C_q's are within a reasonable range of 1.2–4 MHz. A few calculated C_q's are found between 4 and 7.2 MHz, which is on the upper end of known values for ^{43}Ca.[20–24] Only one of 29 sites in triclinic C_3S shows

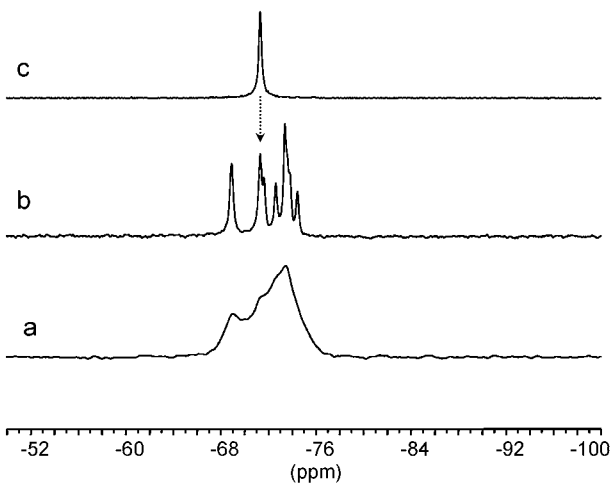

Fig. 2 The ^{29}Si MAS NMR spectra of (**a**) monoclinic C_3S, (**b**) triclinic C_3S and (**c**) β-C_2S. The vertical arrow above the spectrum b indicates the signal of β-C_2S impurity.

unrealistically high calculated C_q of 31.9 MHz. Due to extreme broadening it would be very difficult to verify experimentally if such site is indeed exist. Most likely, however, the discrepancy is due to inaccuracies in the coordinates of one or two oxygen atoms of this complicated structure.[47] The complete set of ^{43}Ca NMR parameters from CASTEP calculations in triclinic C_3S are summarized in Table S1 of the ESI.†

The triclinic C_3S has some impurities of β-C_2S indicated by a signal at about −71.3 ppm in the ^{29}Si spectrum (Fig. 2b compared to Fig. 2c). Considering the ^{43}Ca NMR spectrum of the C_2S (Fig. 1-b), it is suggested that this impurity (which is roughly less than 10 mol.%) is likely to contribute to the ^{43}Ca spectral intensities of triclinic C_3S at about 46 and 29 ppm (Fig. 1c).

C_3A is another component of Portland cement. The ^{43}Ca spectrum of C_3A consists of at least three signals (Fig. 1-e), but possibly even more than that. The region between 100 ÷ 120 ppm appears to show some additional intensity elevated above the noise level, however the overall signal-to-noise ratio is not sufficiently good to state it with certainty. The maxima of intensity for four major signals spread over 100 ppm are found at about 116, 86, 20–40 and 10 ppm The regions are marked as A, B, C and D on Fig. 1-e. The shape of the signals suggests that they are affected by the second order quadrupolar interactions. It is therefore necessary to fit the signals with an appropriate model in order to extract the spectral parameters. The situation, however, is complicated by the fact that we can not be certain if all the sites are resolved in the spectrum. Our attempts to obtain a spectrum at a lower field to constrain the variables were unsuccessful. Due to these deficiencies, the reported in Table 1 quadrupolar parameters need to be considered as working models.

The unit cell of C_3A contains six inequivalent sites for calcium,[59] which can result in six distinct signals in the spectrum if all are resolved. Overlap in the signals can obviously reduce the number of observed components in the spectrum. Larger than average quadrupolar interactions on some sites may also result in broadening of the signals beyond the detection limit. Identification and assignment of signals in C_3A using first principle computations is somewhat problematic too, due to an extremely large size of the unit cell (space group $Pa3$, a = 15,263 Å, $V_{cell} \approx$ 3556 Å^3).[59] The structure is built of six-fold rings centered on three-fold axes and composed of two types of distorted AlO_4 tetrahedra.[59] Two out of six non-equivalent Ca atoms are found on three-fold axes in hexagonal oxygen coordination to one type of oxygen atom in each hexagon. Such symmetry should reflect on the ^{43}Ca signals and result in a characteristic axially symmetric signal with η close to 0. One of the two sites (Ca(1) in notation of ref. 58) forms an octahedron, which is compressed along the threefold axis. The distance between the two planes of O atoms normal to the threefold axis is shorter by 0.64 Å than that for a regular tetrahedron. Such a distortion would immediately result in a substantial quadrupolar constant. The most likely signal for such environment would be that in the region C, with the shape characteristic for η = 0. The isotropic chemical shift and the quadrupolar constant for this site obtained from the fit are then 43.9 ppm and 4.3 MHz. The Ca(2) octahedron is less compressed than that of Ca(1),[59] which would result in a smaller C_q. Considering that the average Ca–O distance in the site Ca(2) is larger than that for the Ca(1) site (2.391 Å compared to 2.338 Å), the isotropic chemical shift of Ca(2) is expected[23,24] to be somewhat smaller than Ca(1). Combining this all together, the region D can be tentatively assigned to the Ca(2). The corresponding NMR parameters for the site are δ_i = 17.0 ppm and C_q = 2.8 MHz. Although the average Ca–O distances for all the sites in the structure are known,[59] the assignment of four remaining Ca sites, however, is hampered by the very limited experimental data available for

Table 1 Experimental and calculated ^{43}Ca NMR parameters in cement based materials

	Calculations (CASTEP)				Experiment, 21.1 T			Structure reference
Compound	σ_i, ppm	$\delta_i^{calc.}$,[a] ppm	C_q, MHz	η	δ_i,[b] ppm	C_q, MHz	η	
CaO	972.6	131.9	0.0	—	136.1	0.0	—	61
$Ca(OH)_2$	1040.7	74.6	2.18	0.0	70.5	2.49	0.1	62
β-C_2S Site 1	1085.8	36.5	2.098	0.66	33.7	2.41	0.65	55
Site 2	1060.4	57.9	2.815	0.43	53.8	2.98	0.7	
Monoclinic-C_3S (36 Ca sites)	—	—	—	—	40 ÷ 110	?	?	47
Triclinic-C_3S (29 Ca sites)[c]	955.6 ÷ 1075.6	44.6 ÷ 145.9	1.2 ÷ 7.2, 31.9	0.02 ÷ 0.95	40 ÷ 140	∼0.5 ÷?	?	46
C_3A (6 Ca sites)	—	—	—	—	17.0	2.8	0.2	58
					43.9	4.3	0.0	
					91.8	2.4	1.0	
					116.9[d]	1.4	0.1	
Tobermorite	1098.5	25.1	2.188	0.77	∼25	?	?	59
	1100.5	23.4	2.303	0.72				
Jennite[e]	1056.5	61.3	2.084	0.51				60
	1072.7	47.6	2.321	0.93				
	1056.2	61.5	1.686	0.98				
	1075.2	45.5	1.953	0.84				
	1077.9	43.2	1.907	0.59				

[a] Converted from the calculated isotropic shielding constants as described in Experimental Part. [b] Referenced to 1 M $CaCl_2$; Estimated errors on the experimental δ_i and C_q are less than 2 ppm and 0.2 MHz, respectively. These errors can be significantly smaller for well defined lineshapes and signals with higher signal-to-noise ratio. [c] See Table S1 of the ESI for a complete list of calculated parameters. [d] See discussion in the text. [e] Multiplicities of Ca sites in Jennite are 2,2,2,2,1.[61]

calcium aluminates, and would be too speculative. The lower symmetry of the oxygen environment for the remaining sites is expected to result in an increased η, which is likely what is observed for the signal in the region B. We note again, that all the assignments reported here for ^{43}Ca of C_3A should be regarded as preliminary. To the best of our knowledge this is a first report of the experimental ^{43}Ca NMR spectrum for C_3A.

One should note that there are very few experimental data on ^{43}Ca shifts between 40 to 110 ppm. A recent paper[24] lists several experimental and calculated isotropic shifts for ^{43}Ca in the range of 40–79 ppm, but (with the exception of CaO) nothing above that. Such significant de-shielding of Ca ions in C_3S and C_3A samples is very difficult to explain and requires further study.

Hydrated cement phases

The ^{43}Ca NMR spectra of synthetic C–S–H phases (C S^{-1} = 0.8, 1.2 and 1.5), 11 Å Tobermorite and hydrated triclinic C_3S are presented in Fig. 3. $Ca(OH)_2$ was also examined as it is one of the hydration products in Portland cement paste.

The signal of calcium hydroxide (Fig. 3-a) clearly shows the effects of the second order quadrupolar interactions in its spectrum. The isotropic chemical shift of 70.5 ppm together with the quadrupolar constant C_q = 2.49 MHz and asymmetry parameter η = 0.1, agree well with previously reported experimental data.[29] Results of the CASTEP calculations of the chemical shift and quadrupolar parameters in the current work for $Ca(OH)_2$ are similar to those recently reported[24] with a slight improvement in the calculated C_q (2.18 MHz *vs.*1.91 MHz in ref. 24).

The hydrated C_3S (Fig. 3-b) has a wide range of broad signals in the region between 20 and 70 ppm. This is not surprising as the main hydration product of C_3S is a nearly amorphous C–S–H which probably has a broad variety of calcium environments. The calcium in the C–S–H structure is located either in the main backbone (on which the silicate tetrahedra are attached) or in the interlayer region (*i.e.* Ca^{2+} ions). It is observed that one signal of relatively higher intensity with an isotropic chemical shift of 69.8 ppm is present in the spectrum. This signal can be accurately assigned to the $Ca(OH)_2$ (in comparison with the spectrum in Fig. 3-a). Calcium hydroxide, the other hydration product of the C_3S in addition to C–S–H, has a crystalline structure. In order to have a better interpretation of the rest of the signals of the hydrated C_3S, the ^{43}Ca NMR spectra of the more-ordered C–S–H systems is examined as follows.

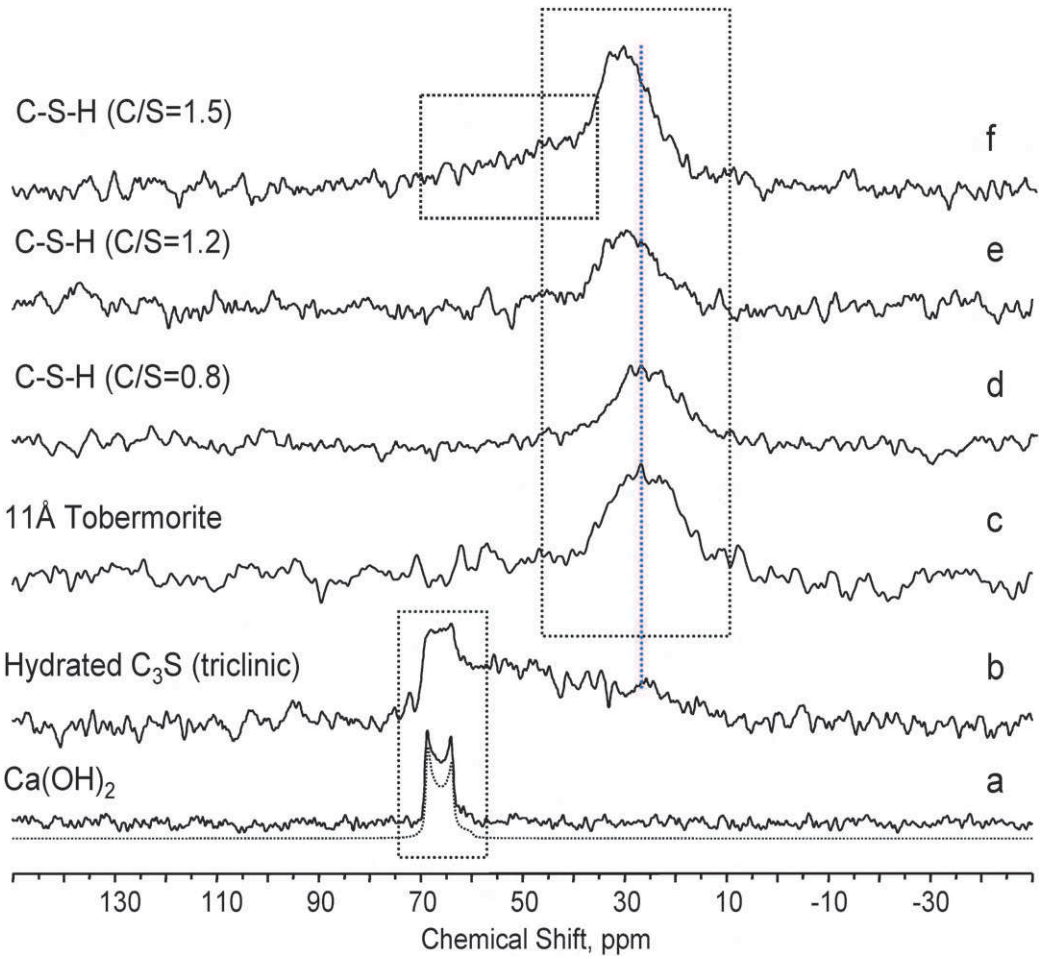

Fig. 3 The natural abundance ^{43}Ca MAS NMR spectra of various C–S–H systems and CH; **a**: calcium hydroxide, **b**: hydrate triclinic C_3S, **c**: 11 Å Tobermorite, and synthetic C–S–H (**d**: C S^{-1} = 0.8, **e**: C S^{-1} = 1.2, **f**: C S^{-1} = 1.5). Dotted line below the spectrum of $Ca(OH)_2$ is the simulation for the second order quadrupolar interactions.

The ^{43}Ca NMR spectrum of 11 Å Tobermorite is shown in Fig. 3-c. It represents a featureless broad signal with the apparent maximum at about 25 ppm. The results of the first principle calculations for 11 Å Tobermorite are summarized in Table 1. The calculations were performed using experimental structure of a so-called anomalous 11 Å Tobermorite, which is a calcium-poor polymorph that is better suited to the composition of the material used in the NMR experiment (space group B 1 1 m, a = 6.735 Å, b = 7.385 Å, c = 22.487 Å, γ = 123.25°).[60] The calculations predict two very close spaced signals with the chemical shifts at about 23 and 25 ppm with moderate quadrupolar constants in a range of 2–2.3 MHz (Table 1). Considering a commonly present dispersion of the chemical shifts and quadrupolar constant in a real sample, one could hardly expect that these two signals will be resolved in an experimental spectrum. In an agreement with the calculations, a rather broad signal has been observed with a maximum at about 25 ppm. We note, that this is significantly different to a maximum at about 0 ppm (after correcting for the difference in the chemical shift of the references) recently reported for 11 Å Tobermorite.[42]

A sample of Jennite was not available for the current study and therefore the experimental ^{43}Ca data is not reported here. The CASTEP calculations performed on a reported structure of Jennite,[61] however, suggest that more than one signal and at significantly different positions than reported recently,[42] should be observed (Table 1). The structure of Jennite is triclinic and contains 5 distinct Ca sites.[61] The calculated isotropic chemical shifts are at 61.3, 61.5, 47.6, 45.5, and 43.2 ppm, with the last signal only at half intensity due to its reduced population in the structure. The corresponding calculated C_q's (η_q's) are 2.08 (0.51), 1.69 (0.98), 2.32 (0.93), 1.95 (0.84), and 1.91 MHz (0.59), respectively. Since the expected quadrupolar constants are smaller than those in β-C_2S, the resulting line broadening due to the second order quadrupolar interactions should be less than in that case. Based on the proximity of their expected isotropic chemical shifts, the sites can be separated into two distinct groups. Considering some overlap of the individual lines and the second order quadrupolar shifts, one should expect a spectrum with two separate signals of slightly different intensities centered at about 50–55 and 30–35 ppm. The calculated chemical shifts for ^{43}Ca using the GIPAW method are usually accurate within ±5 ppm.[20,24] Even if we accept the upper limits of the errors, the computational results predict the spectra notably different from those reported,[42] suggesting some irregularities of the previously published ^{43}Ca spectrum for this mineral.

The ^{43}Ca NMR results of synthetic C–S–H phases (C/S ratios of 0.8, 1.2 and 1.5 presented in Fig. 3-d, 3-e and 3-f, respectively) show relatively broad signals at about 27–31 ppm very similar to that for the 11 Å Tobermorite. In very general terms, this corresponds to Ca in a silicate environment.[23,24] Relatively low intensities of the ^{43}Ca signals from C–S–H samples are due to their comparatively low density as well as the low population of the calcium atoms in the unit volume. It appears that the increase in the C/S ratio results in a slight shift of the location of the main ^{43}Ca signal to more positive chemical shift values (higher frequencies). This means that the calcium atoms are being deshielded in C–S–H as it becomes richer in lime content. It is known that the mean length of the silicate chain (flanked on Ca–O backbone) decreases as the C/S ratio increases.[62] In other words, the density of the electrons (from silicates) in the vicinity of the Ca atoms decreases. This results in less shielding of calcium environment and is thus responsible for higher observed chemical shift values as the C/S ratio increases. It is also noted that the chemical shift range of the low frequency signals in hydrated C_3S includes that of the main signals of all C/S ratio synthetic C–S–H systems. This may suggest that the C–S–H in hydrated cement systems (*e.g.* produced in the hydration of C_3S) can possibly appear in various locally different chemical compositions. It is therefore likely that a mixture of Tobermorite- and Jennite-like phases as proposed before exist in the Portland cement paste.[63]

Another interesting feature is that a broad signal appears as shoulder on the main signal of the C/S = 1.5 C–S–H (Fig. 3-f) at its high frequency side. This range (although more shielded) corresponds to the region of the hydrated C_3S spectrum in which the $Ca(OH)_2$ signal is located. It should be noted that at higher C/S ratios, the synthetic C–S–H contains more calcium ions in the interlayer region. Some free calcium hydroxide may even exist. Considering these points, the relatively broad signal on the shoulder of the main signal in C–S–H (C/S = 1.5) spectrum is assigned to the calcium ions in the interlayer space. To test if we see all the calcium in the samples, the normalized intensities were compared and the dependence of the intensity of signals *versus* the delay time (saturation of the signals) was verified. Indeed, the intensity of normalized signals (to the mass of samples and number of scans) grew proportionally with the increase in the C/S ratios (not shown). Considering the analogies between the synthetic C–S–H and the C–S–H in hydrated C_3S, the ^{43}Ca NMR signals of the hydrated C_3S can be assigned to various calcium environments as shown in Fig. 4.

The minerals Jennite and Tobermorite are often considered as model systems for C–S–H. Recently, an attempt has been made to obtain the ^{43}Ca spectra of these minerals.[42] Although the measurements have been performed at a high magnetic field of 21 T, the obtained spectra are of rather poor quality. Nevertheless, the authors drew some far reaching conclusions. More specifically, they question if Jennite and Tobermorite can be used at all as model systems for C–S–H. According to the ^{43}Ca NMR results of the current study, it is suggested that

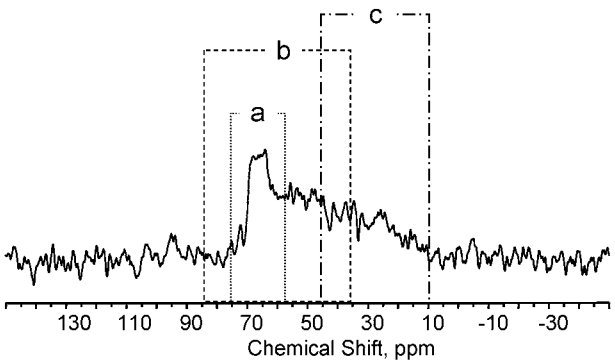

Fig. 4 Approximate ranges of ^{43}Ca NMR chemical shift for various species in hydrated C_3S; (**a**) calcium hydroxide, (**b**) calcium ions in the interlayer space, and (**c**) calcium in the Ca–O backbone.

the synthetic and more-ordered C–S–H systems such as Tobermorite and C–S–H(I) have similar calcium environments and can structurally be considered as model materials for the C–S–H produced in hydrated Portland cement. One should note that the positions of the ^{43}Ca signals in the C–S–H samples are in a good agreement with that previously observed in synthetic C–S–H prepared through double decomposition method[36] (after correction for the difference in the used chemical shift reference).

Conclusions

^{43}Ca solid state NMR remains a challenging task even with the access to the highest available magnetic field. The recent developments in the experimental instrumentation and the advances in computational techniques have progressed the method on the level that makes it suitable and useful in solving the long standing problems of materials sciences. In this work we attempted a systematic ^{43}Ca high field SS NMR study on a series of cement-based materials, aimed at defining the possibilities and the limitations of the method in cement and concrete research. In the first phase of this research we examined the spectra in a number of cement related compounds of known structure and cement research, such as di-calcium silicate (β-C_2S), tri-calcium composition. The spectra of several materials important in silicate (C_3S) silicates, and tri-calcium aluminate (C_3A), were obtained for the first time. The relation of spectroscopic and structural parameters was at the center of the study and the assignment of the signals was assisted by the first principles calculations. The results for the hydrated systems show that the amorphous C–S–H produced in the hydration of C_3S has similar calcium structural features to those for the well-ordered C–S–H phases such as synthetic C–S–H(I) and 11 Å Tobermorite. Although all synthetic C–S–H materials are structurally related to that in hydrated cement paste, the high C S^{-1} ratio C–S–H(I) appears to have a calcium environment more related to that of the amorphous C–S–H in hydrated C_3S. The ^{43}Ca NMR chemical shifts of the hydrated C_3S were assigned to the calcium atoms in the Ca–O backbone and interlayer space of C–S–H in addition to that in the free calcium hydroxide.

Acknowledgements

The authors thank Dr Victor Terskikh for technical assistance and useful discussions. Access to the 900 MHz NMR spectrometer and Accelrys Materials Studio modeling package was provided by the National Ultrahigh Field NMR Facility for Solids (Ottawa, Canada), a national research facility funded by the Canada Foundation for Innovation, the Ontario Innovation Trust, Recherche Québec, the National Research Council Canada, and Bruker BioSpin and managed by the University of Ottawa (http://www.nmr900.ca).

References

1 E. Worrell, L. Price, N. Martin, C. Hendriks and L. O. Meida, *Annu. Rev. Energy Environ*., 2001, **26**, 303.
2 E. Lippmaa, M. Mägi, A. Samoson, G. Engelhardt and A. R. Grimmer, *J. Am. Chem. Soc*., 1980, **102**, 4889.
3 G. Engelhardt, M. Nofz, K. Forkel, F. G. Wihsmann, M. Mägi, A. Samoson and E. Lippmaa, *Phys. Chem. Glasses*, 1985, **26**, 157.
4 E. Lippmaa, M. Mägi, M. Tarmak, W. Wieker and A. R. Grimmer, *Cem. Concr. Res*., 1982, **12**, 597.
5 D. Müller, A. Rettel, W. Gessner and G. Scheler, *J. Magn. Res*., 1984, **57**, 152.
6 J. R. Barnes, A. D. H. Clague, N. J. Clayden, C. M. Dobson, C. J. Hayes, G. W. Groves and S. A. Rodger, Hydration of portland cement followed by ^{29}Si solid-state NMR spectroscopy, *J. Mater. Sci. Lett*., 1985, **4**, 1293.
7 J. Skibsted, E. Henderson and H. J. Jakobsen, *Inorg. Chem*., 1993, **32**, 1013.
8 J. Hjorth, J. Skibsted and H. J. Jakobsen, *Cem. Concr. Res*., 1988, **18**, 789.
9 Y. Tong, H. Du and L. Fei, *Cem. Concr. Res*., 1990, **20**, 986.
10 X. Cong and R. J. Kirkpatrick, *Cem. Concr. Res*., 1993, **23**, 1065.
11 X. Cong and R. J. Kirkpatrick, *Adv. Cem. Based Mater*., 1996, **3**, 133.
12 J. Roncero, S. Valls and R. Gettu, *Cem. Concr. Res*., 2002, **32**, 103.
13 M. D. Andersen, H. J. Jakobsen and J. Skibsted, *Inorg. Chem*., 2003, **42**, 2280.
14 S. L. Poulsen, V. Kocaba, G. LeSaout, H. J. Jakobsen, K. L. Scrivener and J. Skibsted, *Solid State Nucl. Magn. Reson*., 2009, **36**, 32.
15 R. Alizadeh, L. Raki, J. M. Makar, J. J. Beaudoin and I. Moudrakovski, *J. Mater. Chem*., 2009, **19**, 7937.
16 *Application of NMR Spectroscopy to Cement Science*, ed. P. Colombet and A. R. Grimmer, Gordon and Breach Science Publishers, Amsterdam, 1994.
17 *Nuclear Magnetic Resonance Spectroscopy of Cement-Based Materials*, ed. P. Colombet, A. R. Grimmer, H. Zanni and P. Sozzani, Springer, Berlin, 1998.
18 J. Skibsted, C. Hall and H. J. Jakobsen, in *Structure and Performance of Cements*, ed. J. Benstedt and P. Barnes, Spon Press, London, 2002, p. 457.
19 G. Engelhardt and D. Michel, *High-Resolution Solid-State NMR of Silicates and Zeolites*, John Wiley & Sons, Chichester, 1987.
20 D. L. Bryce, E. B. Bultz and D. Aebi, *J. Am. Chem. Soc*., 2008, **130**, 9282.
21 (*a*) D. Laurencin, A. Wong, J. V. Hanna, R. Dupree and M. E. Smith, *J. Am. Chem. Soc*., 2008, **130**, 2412; (*b*) D. Laurencin, C. Gervais, A. Wong, C. Coelho, F. Mauri, D. Massiot, M. E. Smith and C. Bonhomme, *J. Am. Chem. Soc*., 2009, **131**, 13430.
22 K. J. D. MacKenzie and M. E. Smith, *Multinuclear Solid-state NMR of Inorganic Materials*, Pergamon, New York, 2002.
23 R. Dupree, A. P. Howes and S. C. Kohn, *Chem. Phys. Lett*., 1997, **276**, 399.
24 C. Gervais, D. Laurencin, A. Wong, F. Pourpoint, J. Labram, B. Woodward, A. P. Howes, K. J. Pike, R. Dupree, F. Mauri, C. Bonhomme and M. E. Smith, *Chem. Phys. Lett*., 2008, **464**, 42.
25 (*a*) M. Profeta, F. Mauri and C. J. Pickard, *J. Am. Chem. Soc*., 2003, **125**, 541; (*b*) C. Gervais, L. Bonhomme-Coury, F. Mauri, F. Babonneau and C. Bonhomme, *Phys. Chem. Chem. Phys*., 2009, **11**, 6953; (*c*) M. Benoit, M. Profeta, F. Mauri, C. J. Pickard and M. E. Tuckerman, *J. Phys. Chem. B*, 2005, **109**, 6052; (*d*) S. E. Ashbrook, A. J. Berry, D. J. Frost, A. Gregorovic, C. J. Pickard, J. E. Readman and S. Wimperis, *J. Am. Chem. Soc*., 2007, **129**, 13213; (*e*) J. M. Griffin, S. Wimperis, A. J. Berry, C. J. Pickard and S. E. Ashbrook, *J. Phys. Chem. C*, 2009, **113**, 465.
26 H. Zanni, R. Rassembertolo, S. Masse, L. Fernandez, P. Nieto and B. Bresson, *Magn. Reson. Imaging*, 1996, **14**, 827.
27 K. J. D. MacKenzie, M. Schmucker, M. E. Smith, I. J. E. Poplett and T. Kemmitt, *Thermochim. Acta*, 2000, **363**, 181.
28 D. Padro, V. Jennings, M. E. Smith, R. Hoppe, P. A. Thomas and R. Dupree, *J. Phys. Chem. B*, 2002, **106**, 13176.
29 A. Trokiner, A. Bessiere, R. Thouvenot, D. Hau, J. Marko, W. Nardello, C. Pierlot and J. M. Aubry, *Solid State Nucl. Magn. Reson*., 2004, **25**, 209.
30 Z. J. Lin, M. E. Smith, F. E. Sowrey and R. J. Newport, *Phys. Rev. B*., 2004, **69**, 4107, 224107.
31 S. Marchand, A. Trokiner, A. Yakubovsky, A. Knizhnik and Y. Eckstein, *Phys. C*, 2004, **408–410**, 826.
32 K. Shimoda, Y. Tobu, K. Kanehashi, T. Nemoto and K. Saito, *Chem. Lett*., 2005, **34**, 1588.

33 A. Wong, A. P. Howes, R. Dupree and M. E. Smith, *Chem. Phys. Lett*., 2006, **427**, 201.
34 K. Shimoda, Y. Tobu, Y. Shimoikeda, T. Nemoto and K. Saito, *J. Magn. Reson*., 2007, **186**, 156.
35 F. Angeli, M. Gaillard, P. Jollivet and T. Charpentier, *Chem. Phys. Lett*., 2007, **440**, 324.
36 K. J. D. MacKenzie, M. E. Smith and A. Wong, *J. Mater. Chem*., 2007, **17**, 5090.
37 I. C. M. Kwan, A. Wong, Y. M. She, M. E. Smith and G. Wu, *Chem. Commun*., 2008, 682.
38 K. Shimoda, Y. Tobu, K. Kanehashi, T. Nemoto and K. Salto, *J. Non-Cryst. Solids*, 2008, **354**, 1036.
39 H. Pizzala, S. Caldarelli, J.-G. Eon, A. M. Rossi, D. Laurencin and M. E. Smith, *J. Am. Chem. Soc*., 2009, **131**, 5145.
40 R. E. Youngman and C. M. Smith, *Phys. Rev. B: Condens. Matter Mater. Phys*., 2008, **78**, 014112.
41 A. Wong, D. Laurencin, G. Wu, R. Dupree and M. E. Smith, *J. Phys. Chem. A*, 2008, **112**, 9807.
42 G. M. Bowers and R. J. Kirkpatrick, *J. Am. Ceram. Soc*., 2009, **92**, 545.
43 A. Wong, D. Laurencin, R. Dupree and M. E. Smith, *Solid State Nucl. Magn. Reson*., 2009, **35**, 32.
44 D. Laurencin, A. Wong, R. Dupree and M. E. Smith, *Magn. Reson. Chem*., 2008, **46**, 347.
45 D. Freude and J. Haase, in *NMR Basic Principles and Progress*, ed. P. Diehl, E. Fluck, H. Günther, R. Kasfeld and J. Seelig, Springer-Verlag, Berlin, 1993, vol. 29, pp. 1–90.
46 S. E. Ashbrook and M. J. Duer, *Concepts Magn. Reson*., 2006, **28a**, 183.
47 N. I. Golovastikov, P. G. Matveeva and N. B. Belov, *Kristallografia*, 1975, **20**, 721 (Russ.).
48 F. Nishi and Y. Takeuchi, *Zeit. Kristallogr*., 1985, **172**, 297.
49 H. M. Jennings, *Cem. Concr. Res*., 2008, **38**, 275.
50 J. J. Beaudoin and R. Alizadeh, *Cem. Concr. Res*., 2008, **38**, 1026.
51 R. Alizadeh, J. J. Beaudoin, V. S. Ramachandran and L. Raki, *Advances in Cement Research*, 2009, **21**, 59.
52 S. J. Clark, M. D. Segall, C. J. Pickard, P. J. Hasnip, M. J. Probert, K. Refson and M. C. Payne, *Z. Kristallogr*., 2005, **220**, 567.
53 L. Frydman and J. S. Harwood, *J. Am. Chem. Soc*., 1995, **117**, 5367.
54 Accelrys Materials Studio®, v 4.4, www.accelrys.com.
55 J. P. Perdew, K. Burke and M. Ernzerhof, *Phys. Rev. Lett*., 1996, **77**, 3865.
56 K. Mori, R. Kiyanagi, M. Yonemura, K. Iwase, T. Sato, K. Itoh, M. Sugiyama, T. Kamiyama and T. Fukunaga, *J. Solid State Chem*., 2006, **179**, 3286.
57 *NMR Spectroscopy of Cement Based Materials*, ed. P. Colombet, A. R. Grimmer, H. Zanni and P. Sozzani, Springer-Verlag, Berlin, 1998, p. 430.
58 H. F. W. Taylor, *Cement Chemistry*, Thomas Telford, London, 2nd edn, 1997, p. 459.
59 P. Mondal and J. W. Jeffery, *Acta Crystallogr., Sect. B: Struct. Crystallogr. Cryst. Chem*., 1975, **31**, 689.
60 S. Merlino, E. Bonaccorsi and T. Armbruster, *Amer. Mineral*., 1999, **84**, 1613.
61 E. Bonaccorsi, S. Merlino and H. F. W. Taylor, *Cem. Concr. Res*., 2004, **34**, 1481.
62 X. Cong and R. J. Kirkpatrick, *Adv. Cem. Based Mater*., 1996, **3**, 144.
63 H. F. W. Taylor, *J. Am. Ceram. Soc*., 1986, **69**, 464.